

The Microphysical Structure of Anvil Cirrus: Three Cases from ARM 1994

*K. A. Hilburn and M. R. Poellot
Department of Atmospheric Sciences
University of North Dakota
Grand Forks, North Dakota*

*W. P. Arnott
Atmospheric Science Center
Desert Research Institute
Reno, Nevada*

Introduction

In situ microphysical measurements were made of three cirrus anvils by the University of North Dakota Citation aircraft during the Atmospheric Radiation Measurement (ARM) Remote Sensing Intensive Operational Period (IOP) in April 1994 at the Southern Great Plains (SGP) site. The microphysical data have been analyzed to better understand the particle size distributions, ice water contents (IWC), and ice crystal habits of these clouds. These parameters are important to the proper modeling of cirrus and their radiative effects. We also characterize the inhomogeneity of the anvil cirrus since this may be important in testing parameterizations.

Methodology

The cloud microphysical observations were obtained with a particle measuring system (PMS) Forward Scattering Spectrometer Probe (FSSP), PMS two-dimensional cloud (2DC) optical array probe, and a formvar replicator supplied by the Desert Research Institute (DRI). The 2DC was used to size and count the larger ice particles ($D > 80 \mu\text{m}$), and the FSSP was used to size and count the smaller ice particles ($D < 50 \mu\text{m}$). IWC was computed from the 2DC data using the automated procedure described in Heymsfield and Parrish (1979). Detailed information about ice crystal habit was obtained by the replicator. The replicator captures particles on formvar-coated 16-mm film. The replicator analysis was performed by DRI, and due to the slow and labor-intensive nature of the analysis, a limited number of 10-s and a couple of 60-s intervals were chosen for processing.

Sampling consisted predominantly of Eulerian spirals. This strategy was employed to make comparisons with ground-based observations, but the nonzero environmental wind velocity resulted in the collection of slantwise cloud profiles rather than true vertical cloud profiles. The displacement from a true vertical profile may limit the discussion of vertical microphysical structure because of cirrus inhomogeneity.

Data

The data presented here were collected on April 24 (second flight of the day), April 25, and April 29, and are summarized in Table 1. A cold front was responsible for the thunderstorm activity that created the cirrus sampled on April 24 and April 25. The cirrus sampled on April 24 had been orphaned from the parent convection and had drifted approximately 6 hours (400 km) before being sampled, as the satellite images in Figure 1 show. The cirrus sampled on April 25 was part of a large anvil and had traveled about 3 hours (200 km) before being sampled, as the satellite images in Figure 2 show. Widespread precipitation with imbedded convection was present on April 29 in association with a stationary front. The cirrus sampled for the majority of the flight had traveled for 2 hours (300 km); but as Figure 3 shows, a strong line of thunderstorms developed just to the south of the Cloud and Radiation Testbed (CART) site, and the cirrus sampled during the last spiral-down was only about 20 minutes old (traveling 50 km).

Table 1. A summary of the anvils sampled for this study.

Day April 1994	Flight Pattern	Temperature Range (°C)	Number of Replicator Samples	Description (age, distance traveled)	Average Ice Water Path, gm ⁻²
24, 2nd flight	Spiral-Up	-21 to -58	8	6 hours, 400 km	243.4
25	Spiral-Up	-25 to -61	1	3 hours, 200 km	103.87
	Spiral-Down	-21 to -60	6	3 hours, 200 km	207.52
	Spiral-Up	-26 to -51	0	3 hours, 200 km	173.77
	Spiral-Down	-31 to -51	0	3 hours, 200 km	167.88
29	Climb-Up	-50 to -56	0	2 hours, 300 km	--
	Spiral-Down	-51 to -55	1	2 hours, 300 km	--
	Step Climb	-48 to -57	11	2 hours, 300 km	--
	Spiral-Down	-28 to -58	3	20 minutes, 50 km	218.99

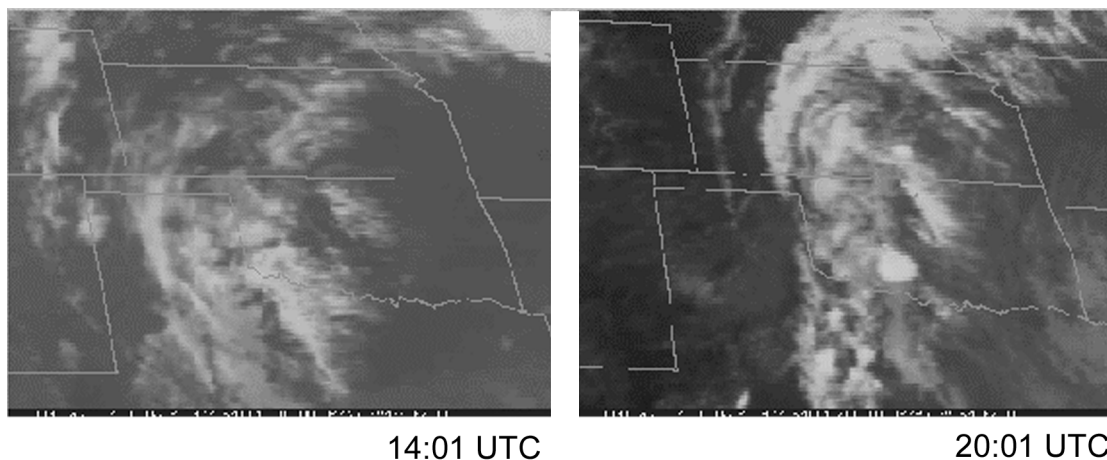


Figure 1. Infrared (IR) satellite for April 24, 1994. The CART site is marked with a square.

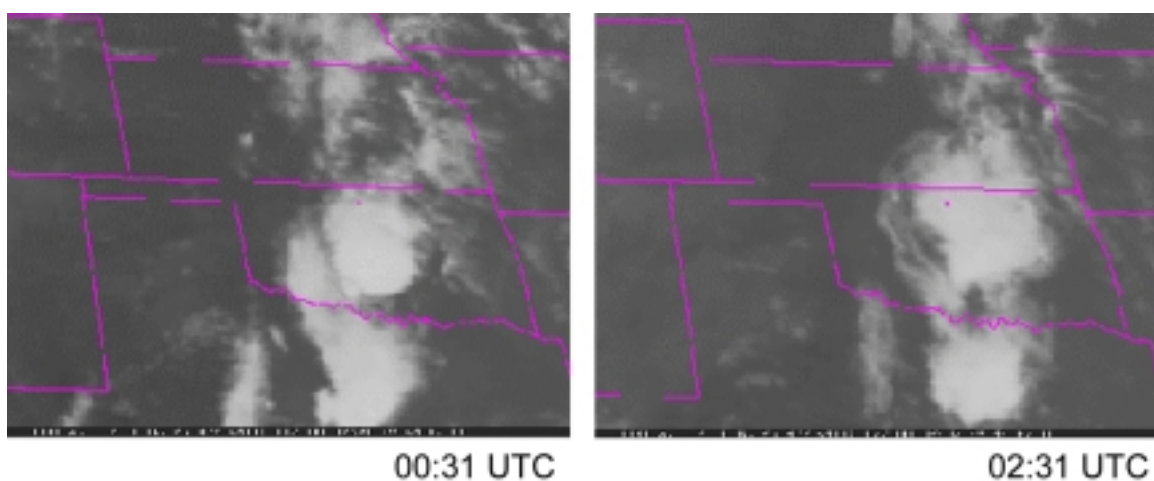


Figure 2. IR satellite for April 25, 1994. The CART site is marked with a square.

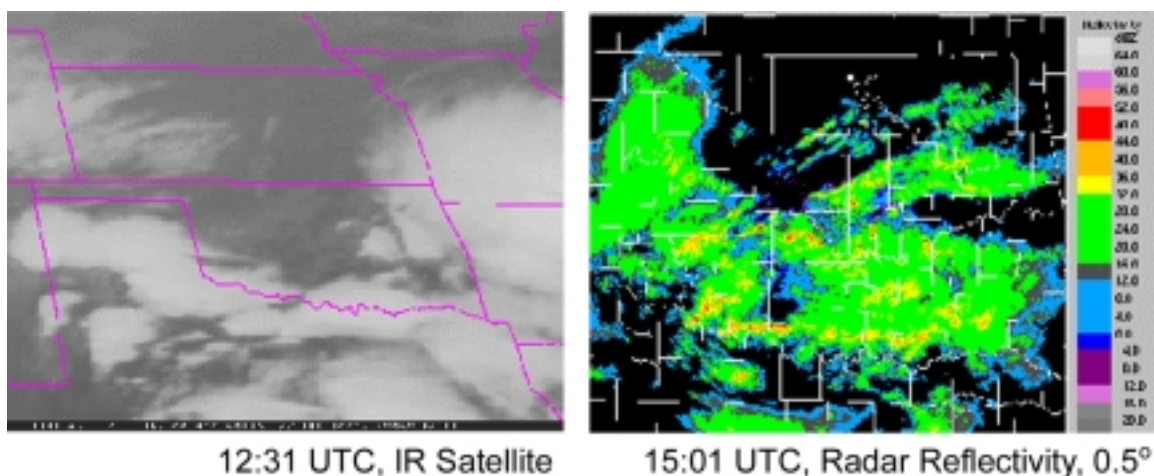


Figure 3. Satellite and radar for April 29, 1994. The CART site is marked with a square.

Results/Discussion

Particle Size Distributions

Figure 4 shows the particle size distributions for April 24, April 25, (1st spiral-down), and April 29 (2nd spiral-down) averaged over 5°C layers. Spectra on all three days exhibit the general trend of fewer small particles and more large particles with increasing temperature. This trend is consistent with sedimentation and with aggregation. Spectra on all three days show a peak in the number density in the neighborhood of 20 μm, and nearly all of the spectra for the three days contain a shoulder in the 100-μm to 300-μm region. All but the coldest spectra on April 24 and April 25 (<-50°C) seem to contain a distinct jump between 52 μm and 82 μm—between the FSSP and 2DC measured portions of the spectrum—suggesting that the FSSP may be overestimating and/or the 2DC may be underestimating.

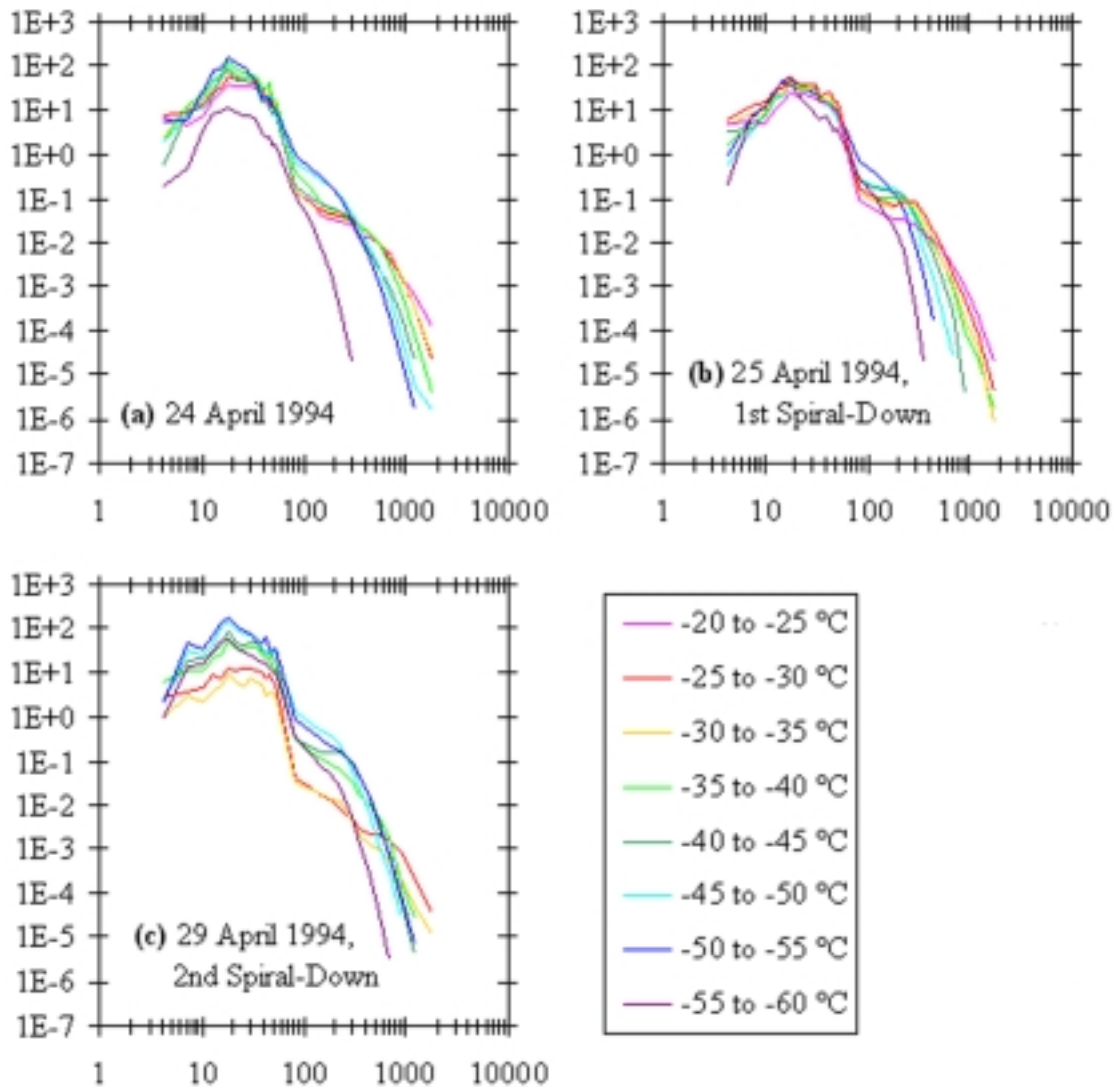


Figure 4. Temperature averaged particle size distributions. Concentration ($L^{-1} \mu m^{-1}$) versus diameter (m).

In order to draw comparisons with other studies, we have computed the total concentration in the portion of the ice particle spectrum measured by the 2DC. Figure 5 shows vertical profiles of 2DC concentration. The greatest concentrations of ice particles were found in the upper portions of the anvils. $5^{\circ}C$ layer average 2DC concentrations were generally on the order of tens per liter, but reached as high as $124 L^{-1}$ on April 29—the freshest cloud in this study.

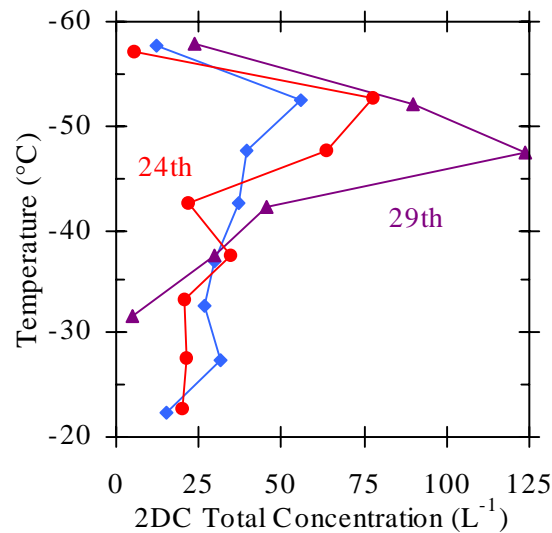


Figure 5. 2DC concentration as a function of temperature.

Cloud Probe Response

The particle size distribution measurements made during the step climb on April 29 give us the opportunity to compare the FSSP, 2DC, and replicator in a region of cloud where large ice particles were absent (measurements were taken at temperatures below -53°C). Two 60-s portions of replicator data along with the corresponding FSSP and 2DC data are given on Figure 6. The 2DC spectra do not contain prominent 100- μm to 300- μm plateaus—similar to the coldest spectra on April 24 and April 25. The replicator spectra suffer a pronounced roll-off for diameters less than 50 μm . We also note an apparent 2DC undercounting for diameters roughly greater than 100 μm . Arnott et al. (1994) found that larger particles (>200 μm) collected by the replicator suffered impaction enlargement of about 4/3. Because the particle concentration increases with decreasing diameter, this enlargement would lead to replicator overcounting and thus to the apparent 2DC undercounting. The concentrations measured by the FSSP are not dissimilar to the FSSP concentrations measured during the spirals (Figure 4) even though the spirals contained much larger particles. Extrapolation of the 2DC data to smaller particle sizes (down to 20 μm) yields concentrations similar to those measured by the FSSP. This suggests that the FSSP concentrations may not be overestimating as badly as thought, but without other probes overlapping the FSSP and 2DC portions of the spectrum, it is difficult to draw conclusions.

Ice Water Content

Figure 7 shows the 2DC IWC as a function of temperature for the three days. We would expect that sedimentation and aggregation would lead to a vertical profile where IWC increased with increasing temperature except perhaps at the lowest level of the cloud where ice mass might evaporate. Such a profile was observed in the moderately aged cirrus on April 25. The cloud on April 24 is multi-layered, possibly the result of upper-level ascent, but uncertainties in measuring vertical velocity in a spiral and a

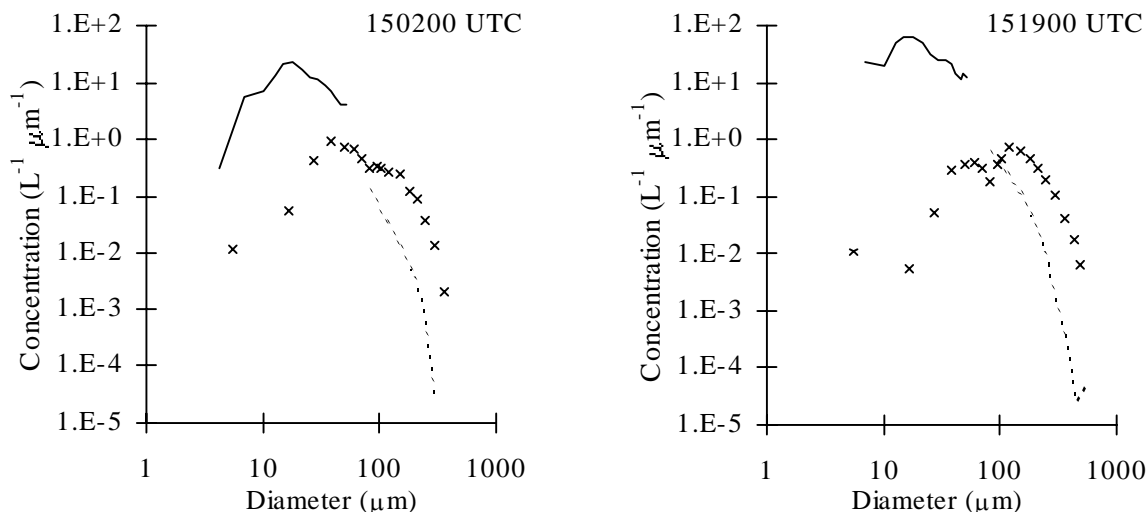


Figure 6. Particle size spectra measured by the FSSP (line), replicator (x's), and 2DC (dashed line) on April 29.

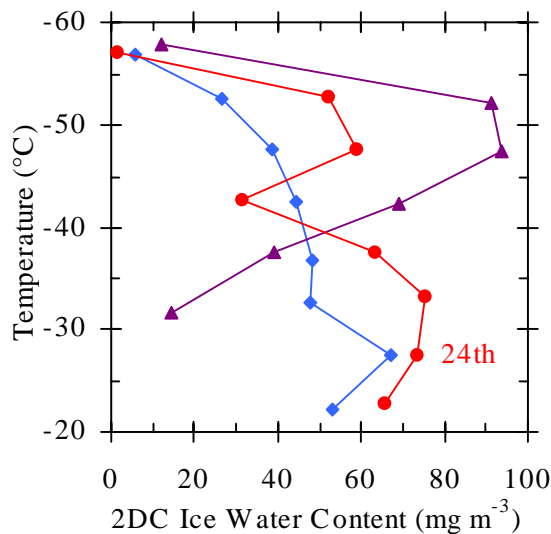


Figure 7. 2DC IWC as a function of temperature.

lack of frost point data on this flight prevent us from drawing a conclusion. The cirrus sampled on April 29 contained some of the highest average values of IWC for the three days. The high center of mass in the April 29 anvil cloud seems consistent with the proximity of convection (within 50 km). Ice crystals that had been lofted high into the troposphere had not had enough time to sediment to lower levels.

Ice Crystal Habit

The replicator processing classified ice crystals into one of five types: column, plate, polycolumn, polyplate, and miscellaneous. Examples of these crystal types (as captured by the replicator) are given in Figure 8. Figure 9a gives vertical (temperature) profiles of ice crystal habit for April 24 and April 25. The anvils were rich in plate polycrystals on both days, with one notable exception shown in Figure 9a where column polycrystals predominate. This sample contains 308 crystals, which makes it unlikely that this was a sampling anomaly. If the multi-layered structure of the April 24 IWC profile was due to upper-level ascent, this could help explain the polycolumns because crystal growth at that temperature would be of columnar form.

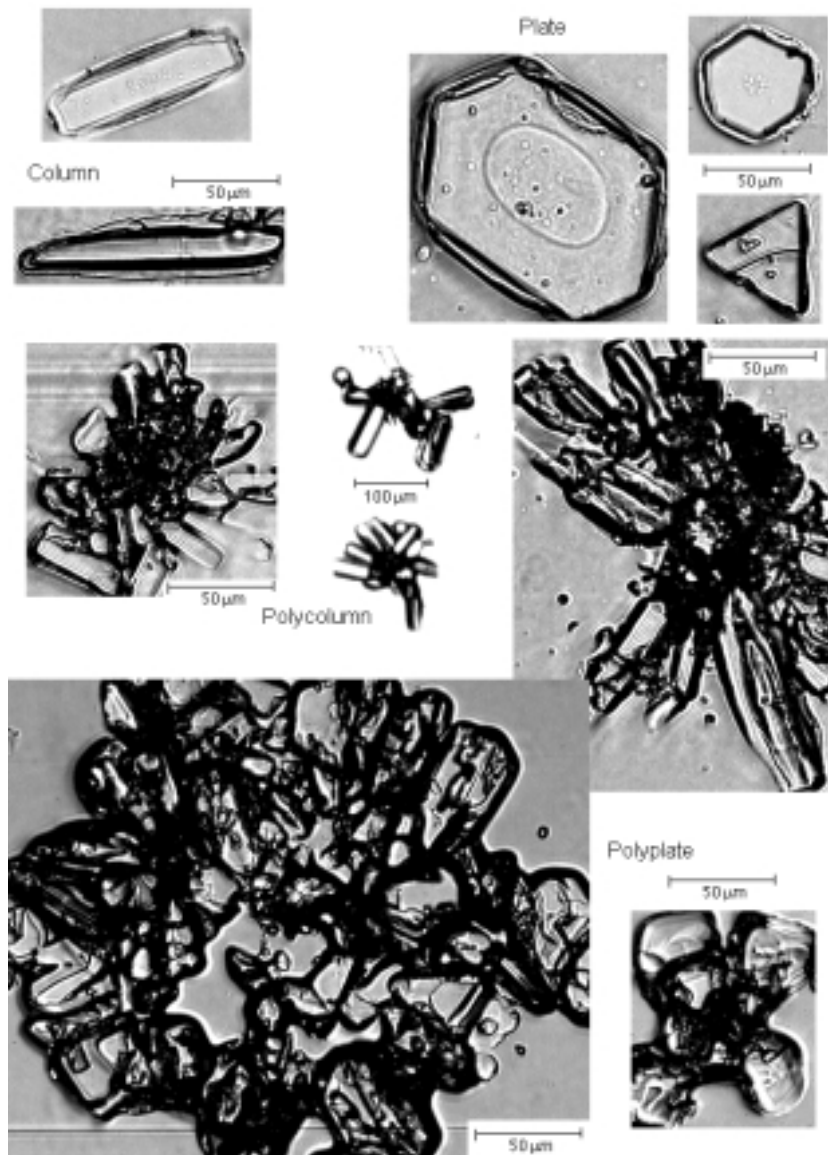


Figure 8. Examples of replica for different habit types.

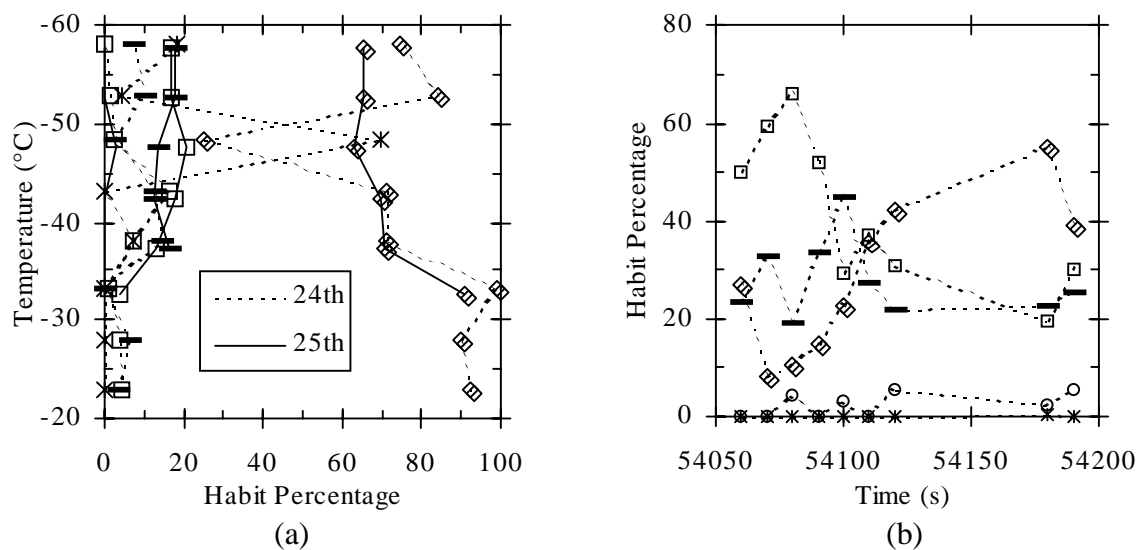


Figure 9. Replicator habit percentage with columns, plates, polycolumns, polyplates, and miscellaneous given by bars, squares, asterisks, double diamonds, and circles, respectively.

All of the replicator data for April 29 were taken between -45°C and -60°C . Most of the data were taken during a 140-s period during the step-climb where eight 10-s intervals and one 60-s interval were analyzed. The habit percentage as a function of time is given by Figure 9b. The aircraft ascended 157 m during this segment. Although the first six samples contain few crystals (30, 37, 47, 27, 31, and 59 crystals, respectively), which prevents making inferences about habit inhomogeneity, it is clear that monocrystalline forms were relatively more abundant than polycrystals in this (the upper) portion of the April 29 anvil.

Mesoscale Inhomogeneity

The four spirals flown over a two-hour time period on April 25 give us the opportunity to examine the mesoscale inhomogeneity in the anvil. We must be careful not to interpret micro (10^0 -km) scale inhomogeneity as meso- γ (10^1 -km) scale inhomogeneity. That is, large fluctuations over small distances could potentially mask larger-scale trends. To avoid this problem, we have averaged the data over the top, middle, and bottom thirds of the anvil cloud. We have chosen to define cloud top and bottom from the in situ observations made by the Citation.

Figure 10a shows the 2DC IWC for the four different spirals. As one might expect, the values of IWC at the tops of the first spiral-up and first spiral-down and the tops of the second spiral-up and second spiral-down are similar. The values of IWC at the bottom of the first spiral-down and second spiral-up were not overly similar, and in fact, the change in IWC in the bottom layer is not monotonic in time. Between spirals, not only does the maximum value of IWC change, but also the position at which this maximum is located changes. As the cloud drifts over the sampling area with time, the maximum IWC moves from the middle of the cloud, to the bottom, back to the middle, and back to the bottom of the cloud. The larger-scale structure of the anvil cloud is not homogeneous, as though the ice crystals were

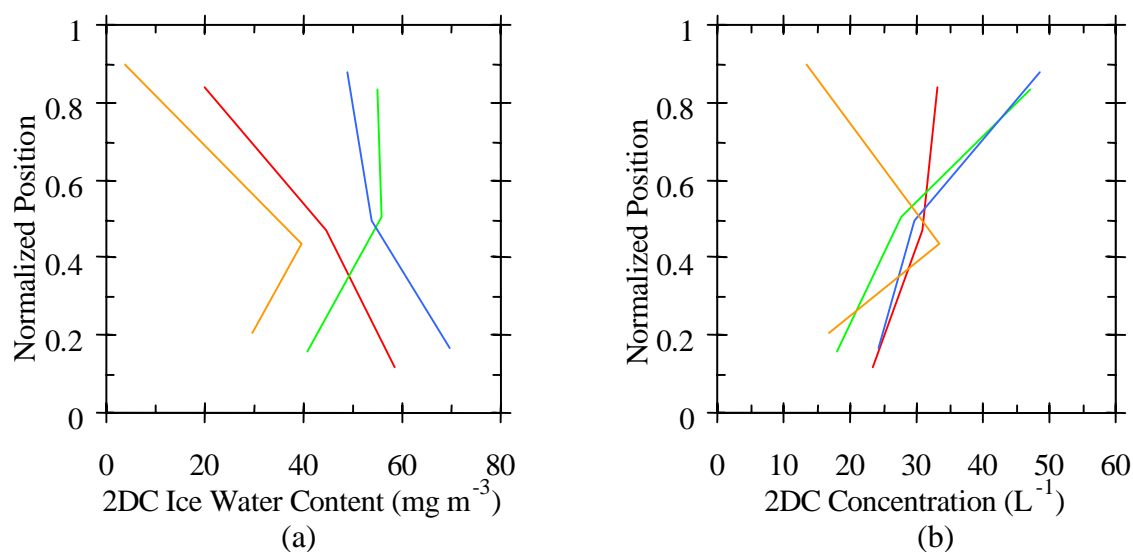


Figure 10. 2DC IWC and concentration as functions of position for the first spiral-up, first spiral-down, second spiral-up, and second spiral-down, which are marked with orange, red, green, and blue curves, respectively.

continually lofted in a steady stream by a smokestack; instead the large-scale structure displayed more of a pulsing character. We note that the middle of the cloud seems the most homogeneous with the top showing the most variation. Figure 10b shows that as time passed, the 2DC concentration increased in the top of the cloud. 2DC concentration in the middle and bottom of the cloud oscillated without monotonic behavior.

Conclusions

Three anvils sampled as part of ARM 1994 allowed us to document the structure of aged, mid-latitude, continental anvil cirrus. The average 2DC IWC and 2DC concentration in anvils sampled from 50 km to 400 km downwind ranged over an order of magnitude, and the larger scale structure of the April 25 anvil seemed to display a pulsing character. Particle size distributions contained similar features on all three days such as a mode near $20 \mu\text{m}$ and a plateau in the $100\text{-}\mu\text{m}$ to $300\text{-}\mu\text{m}$ region. Plate polycrystals were the predominant habit in the anvil sampled on April 24 and 25, but monocrystals were also prevalent in the anvil sampled on April 29.

Acknowledgments

This work was supported under U.S. Department of Energy (DOE) Grant #DE-FG03-97ER62360 (Poellot and Hilburn) and #DE-FG03-97ER62399 (Arnott).

Corresponding Author

M. R. Poellot, 701-777-3180, poellot@aero.und.edu

References

Arnott, W. P., Y. Dong, J. Hallett, and M. R. Poellot, 1994: Role of small ice crystals in radiative properties of cirrus: A case study, FIRE II, November 22, 1991. *J. Geophys. Res.*, **99**, 1371-1381.

Heymsfield, A. J., and J. Parrish, 1979: Techniques employed in the processing of particle size spectra and state parameter data obtained with the T-28 aircraft platform. NCAR/TN-137+1A, National Center for Atmospheric Research, Boulder, Colorado.